Journal of Structural Biology **137,** 31–40 (2002)
doi:10.1006/jsbi.2002.4449

# Analysis of the Collagen VI Assemblies Associated with Sorsby's Fundus Dystrophy

Carlo Knupp,* N. H. Victor Chong,† Peter M. G. Munro,† Philip J. Luthert,† and John M. Squire*

**Biological Structure and Function Section, Biomedical Sciences Division, Imperial College Faculty of Medicine, London SW7 2AZ, United Kingdom; and †Department of Pathology, Institute of Ophthalmology, University College London, London EC1V 9EL, United Kingdom*

Received November 29, 2001

**Age-related macular degeneration is the leading cause of blindness in the Western world, and the pathophysiology of the condition is largely unknown. However, it shares many clinical and pathological features with Sorsby's fundus dystrophy (SFD), an autosomal dominant disease, known to be associated with mutations in the *TIMP-3* gene. In Bruch's membrane of both conditions, there are molecular assemblies with distinct transverse bands occurring with a periodicity of about 100 nm. Similar assemblies were also found in the vitreous of a patient with full-thickness macular holes and were identified as being made of collagen VI. The assemblies found in the eye with SFD can be classified into two types, both with a 105-nm axial repeat, but one showing pairs of narrow bands about 30 nm apart and the other showing a single broad band in every repeat. By comparison with the assemblies in the vitreous, collagen VI is considered to be the most likely protein in these assemblies. Furthermore, both of the assemblies associated with SFD can be explained in terms of collagen VI tetramers, one in which the tetramers bind to the mutant tissue inhibitor of metalloproteinases-3 (the gene product of *TIMP-3*) and the other in which little or no binding occurs. TIMP-3 bound to collagen VI may be more resistant to degradation and create an imbalance between the normal amount of TIMP-3 and matrix metalloproteinases (the substrate of TIMPs) in Bruch's membrane with consequent disruption of the normal metabolic processes. Understanding the structure of these collagen VI/TIMP assemblies in Bruch's membrane may prove to be important for understanding the pathophysiology of age-related macular degeneration.** 

***Key Words:*** **collagen VI; blindness; macula; Bruch's membrane; age-related macular degeneration (AMD); Sorsby's fundus dystrophy (SFD); network forming collagens.**

## INTRODUCTION

The clinical and pathological features of Sorsby's fundus dystrophy (SFD), an autosomal dominant condition, are in many ways similar to age-related macular degeneration. Age-related macular degeneration is the leading cause of irreversible blindness in developed countries. Both conditions involve Bruch's membrane, and, although Sorsby's fundus dystrophy is characterized by earlier onset, pathological changes in Bruch's membrane are common in aging and age-related diseases (Hageman, 1997; Marshall *et al.,* 1998; Guymer and Bird, 1998).

Bruch's membrane is a trilaminar extracellular matrix complex that lies between the retinal pigment epithelium and the choriocapillaris, which is the primary capillary bed of the choroid. Bruch's membrane comprises inner and outer collagenous layers that sandwich a central region composed largely of elastin. The strategic location of Bruch's membrane between the outer retina and its primary source of nutrition, the choroidal vasculature, makes it essential for normal retinal function.

Documented age-related changes of Bruch's membrane include progressive thickening (Feeney-Burns and Ellersieck, 1985; Bird, 1992; Newsome *et al.,* 1987a,b; Ramrattan *et al.,* 1994), accumulation of lipids and other extracellular material (Pauleikhoff *et al.,* 1990, 1992; Sheraidah *et al.,* 1993; Holz *et al.,* 1994a,b), changes in the degree of calcification and fragmentation (Spraul and Grossniklaus, 1997), modification and degeneration of collagen and elastin (Feher and Valu, 1967), an increase in advanced glycation end products (Ishibashi *et al.,* 1998), an increase in the amount of noncollagenous proteins (Hewitt *et al.,* 1989; Karwatowski *et al.,* 1995), and deposition of drusen, basal laminar deposits, and basal linear deposits.

Although many of the changes occurring in Bruch's membrane are well described, the mecha-



1047-8477/02 $35.00

nisms by which they lead to the apparent retention of lipids and proteins are not understood nor are the consequences of the deposition process to the etiology of age related-macular degeneration. Functionally, we know that these processes are associated with an exponential reduction in the hydraulic conductivity of Bruch's membrane with age (Moore *et al.*, 1995; Starita *et al.*, 1996; Hodgetts *et al.*, 1998a,b), which, intuitively, must impair normal function of the interface between retinal pigment epithelium and Bruch's membrane.

Extracellular matrix turnover is controlled, at least in part, by the regulated secretion of members of a family of matrix metalloproteinases (MMPs) and their inhibitors, the tissue inhibitors of metalloproteinases (TIMPs). The MMP family of enzymes contributes to both normal and pathological tissue remodeling. A delicate balance of expression and activation, and regulation of TIMP levels, governs the level of destruction mediated by MMPs. Excessive or inappropriate expression of MMPs may contribute to the pathogenesis of many tissue destructive processes, including diseases such as arthritis, multiple sclerosis, atherosclerosis, and chronic obstructive pulmonary disease.

Little is known about the processes that regulate extracellular matrix turnover in Bruch's membrane and the choroid. Retinal pigment epithelium cells secrete the 72- and 92-kDa type IV collagenases, stromelysin, and TIMP-1 *in vitro* (Opdenakker and Van Damme, 1992). MMP-2 and MMP-9, two metalloproteinases with elastolytic properties, increase in Bruch's membrane with age (Guo *et al.*, 1997). TIMP-3 has been shown to be synthesized by retinal pigment epithelium and choroidal endothelial cells and is found at relatively high concentrations in Bruch's membrane and drusen (Vranka *et al.*, 1997). Thus, TIMP-3 may play a major role in maintaining extracellular matrix homeostasis in Bruch's membrane.

Sorsby's fundus dystrophy is linked to the TIMP-3 locus and the responsible mutations of this gene have been identified and characterized (Weber *et al.*, 1994; Felbor *et al.*, 1995; Jacobson *et al.*, 1995; Langton *et al.*, 2000). Mutations in Sorsby's fundus dystrophy result in a substitution that causes incorporation of an additional cysteine residue and hence inappropriate disulfide bridge formation. The most common Sorsby's fundus dystrophy mutation is the Ser181Cys mutation. The mutant protein is thought to cause formation of a TIMP-3 dimer, which may be resistant to normal mechanisms of turnover (Langton *et al.*, 1998) and ultimately give the abnormal accumulation of TIMP-3 demonstrated by immunohistochemistry (Fariss *et al.*, 1998, Chong *et al.*, 2000). This mutant protein was found to retain its metalloproteinase inhibiting activity and the ability to bind to the extracellular matrix (Langton *et al.*, 1998), so its contribution to the pathogenesis of the disease is presumably via a mechanism other than loss of function.

In the normal eye, TIMP-3 immunoreactivity is seen in Bruch's membrane (Fariss *et al.*, 1997; Chong *et al.*, 2000), with transcription localizing mainly to the retinal pigment epithelium and choroid (Ruiz *et al.*, 1996; Vranka *et al.*, 1997). Western blot analysis and reverse zymography have been used to show an increase in protein expression and activity with normal aging (Kamei and Hollyfield, 1999). An accumulation of the TIMP-3 protein in Bruch's membrane of eyes suffering from age-related macular degeneration has been demonstrated by immunohistochemistry (Fariss *et al.*, 1997), and a similar accumulation has been seen in Sorsby's fundus dystrophy (Fariss *et al.*, 1998; Chong *et al.*, 2000).

In the present study we concentrate on the banded assemblies seen in Bruch's membrane. Assemblies of this kind were also seen in the cortical vitreous of a patient with full-thickness macular holes (Knupp *et al.*, 2000). Structurally, these assemblies were characterized by a pattern of pairs of transverse bands, about 30 nm apart, which repeated axially with a periodicity of about 100 nm. A three-dimensional reconstruction of these assemblies, along with considerations of the absolute and relative dimensions of their features, allowed us to identify collagen VI as the most probable component forming them. Collagen VI is a rod-like molecule about 105 nm long with two globular domains at the extremities (Furthmayr *et al.*, 1983). Collagen VI monomers are normally assembled first into antiparallel dimers and then into tetramers which are successively secreted (Ayad *et al.*, 1994). The monomers associate with a 30-nm axial shift. The antiparallel dimers consist of an inner thick rod-like region, 75 nm long, and two shorter (30 nm) and thinner rod-like segments emerging axially from the inner region (Furthmayr *et al.*, 1983). The globular ends of the two monomers are positioned along this structure at the extremities of the inner region and outer segments. Dimers can associate via their 30-nm-long outer segments to form tetramers (Furthmayr *et al.*, 1983; Von der Mark *et al.*, 1984). Artificially cleaved globular terminals join linearly, side by side, to form a necklace whose beads are represented by the N and C terminals, one type connected to the other (Kuo *et al.*, 1995). Tetramers interact to form long chains (Bruns, 1984). Dimers, tetramers, and polymeric chains all have in common a 30-75-30 nm spacing between the globular ends (Furthmayr *et al.*, 1983; Von der Mark *et al.*, 1984; Wu *et al.*, 1987).

Sequence analysis in the triple-helical region of Type VI collagen suggests the likely origin of antiparallel dimer formation (Knupp and Squire, 2001).

## MATERIALS AND METHODS

The eyes of a 77-year-old white woman with SFD caused by the Ser181Cys *TIMP-3* mutation were obtained *postmortem*. Details of this case have been previously published (Fariss *et al.*, 1998; Chong *et al.*, 2000). The right eye was fixed in 0.25% glutaraldehyde and 4% para-formaldehyde in phosphate-buffered saline. Specimens for electron microscopy were postfixed in osmium tetroxide, processed through ascending concentrations of ethanol, and finally infiltrated with Araldite resin. Ultrathin sections were collected on copper grids, sequentially stained in uranyl acetate and lead citrate, and examined in a Jeol 1200 EX transmission electron microscope operating at 80 kV. The assemblies found in the vitreous of a patient with full-thickness macular holes were processed as described in Knupp *et al.* (2000).

Numerous images were taken in the microscope at a calibrated magnification of 15 000 times. Several tilt series were also taken around a tilt axis that was parallel to the broad transverse bands of some of the aggregates in the eye suffering from Sorsby's fundus dystrophy. This was done to correlate the various appearances seen in the microscope. Similarly, tilt series were taken along a tilt axis perpendicular to the broad transverse bands, to check if it was possible to distinguish ordered appearances in the assemblies or to convert one appearance into the other.

The micrographs were digitized with a Leaf-scanner 45 scanner at a resolution of 20 $\mu$m per pixel and examined on a Compaq XP1000 Unix workstation using in-house-developed programs and the MRC (Crowther *et al.*, 1996) program suite. Fourier transforms were calculated and then masked and floated as described by Misell (1978). Figures were prepared on a PC using CorelDraw.

## RESULTS

Figure 1a shows the typical appearance of the molecular aggregates associated with Sorsby's fundus dystrophy. These aggregates form patches of different sizes that extend as clusters. Typically, the aggregates are about 1 $\mu m^2$ in size and are characterized by transverse bands of protein density that repeat axially with a periodicity of approximately 80 to 110 nm. The width of these bands is about 20 to 40 nm. Bands of smaller widths are generally accompanied by smaller axial periodicity, while larger bands are found at axial periodicities of 100–110 nm. Axially, filaments of protein density can be seen, but it is not possible to recognize any regularity in their occurrence. Some of these aggregates (Fig. 1b) differ slightly from those described above since the transverse bands are split into pairs, but they resemble very closely the collagen VI assemblies found in patients suffering from full-thickness macular holes (Knupp *et al.*, 2000; Reale *et al.*, 2001).

The aggregates associated with Sorsby's fundus dystrophy are not highly ordered laterally. Since this is essential for a two- or three-dimensional analysis, we limited our structural study to one dimension.

Initially we carried out a comparison of the Sorsby's fundus dystrophy aggregates with the collagen VI assemblies found in human vitreous (Knupp *et al.*, 2000).

The top panel of Fig. 2a represents a portion of a relatively well-ordered collagen VI assembly in the vitreous. The main axis of the assembly is oriented horizontally for convenience while making the figure. A Fourier transform of this image was calculated and the meridional spots were floated and back Fourier transformed to generate the average in the middle panel of Fig. 2a. This average shows very clearly the double bands that are characteristic of the collagen VI assemblies. These bands are thought to be generated by the transverse alignment of the N and C globular domains of collagen VI dimers and tetramers (Knupp *et al.*, 2000). The pairs of bands occur with a periodicity of about 100 nm. Within the pairs, the bands are about 30 nm apart. In the bottom panel of Fig. 2a, the average protein density from the middle panel is projected onto the *x*-axis. Peaks correspond to higher protein density, and it is possible to see clearly the double-band character of the protein distribution, projected as double-crested peaks. Figure 2b is the result of the analysis carried out on an aggregate found in the eye suffering from Sorsby's fundus dystrophy that shows the double-banding pattern. The top panel represents the raw image. The middle panel is the one-dimensional average of the raw image and the bottom panel is the projection onto the *x*-axis of the protein densities from the average. Figure 2c represents the typical appearance of a single-banded aggregate found in the eye affected by Sorsby's fundus dystrophy. The top panel is the raw image. The middle panel is the averaged image and the bottom panel the projected protein densities. The axial periodicity of the three different structures in Fig. 2 is the same. All the images are shown at the same absolute magnification in the electron microscope without adjustment. The axial features of the aggregates in Figs. 2a and 2b are substantially the same. The better order found in the assemblies in the vitreous (Fig. 2a) yields a better resolution in the averaged image, with a consequent increase in the richness of detail. The dimensions of the double bands that are found in both assemblies match very well: the ratio between the distance separating pairs of bands and bands within the pair is the same for both structures. The aggregate in Fig. 2c does not present double bands, but the width of the single bands is the same as that of double bands, as if the space within the double bands was somehow filled.

Although the aggregates were poorly ordered and

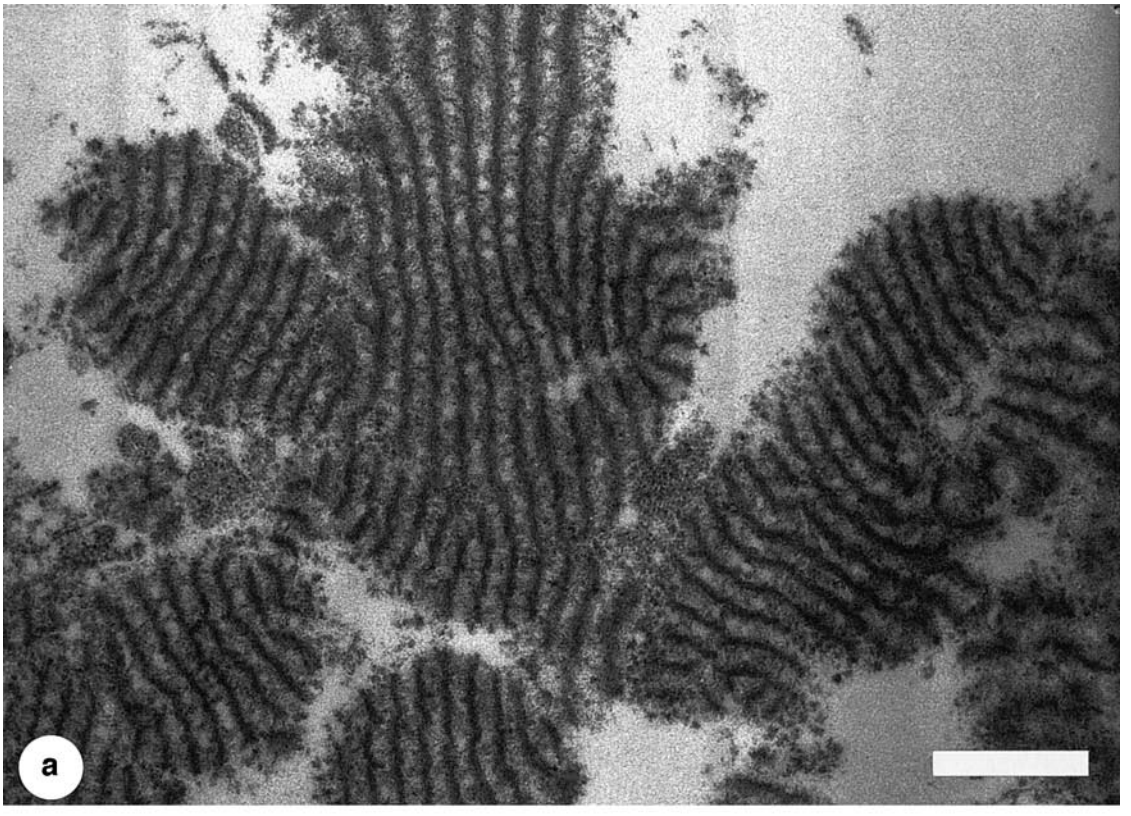
a

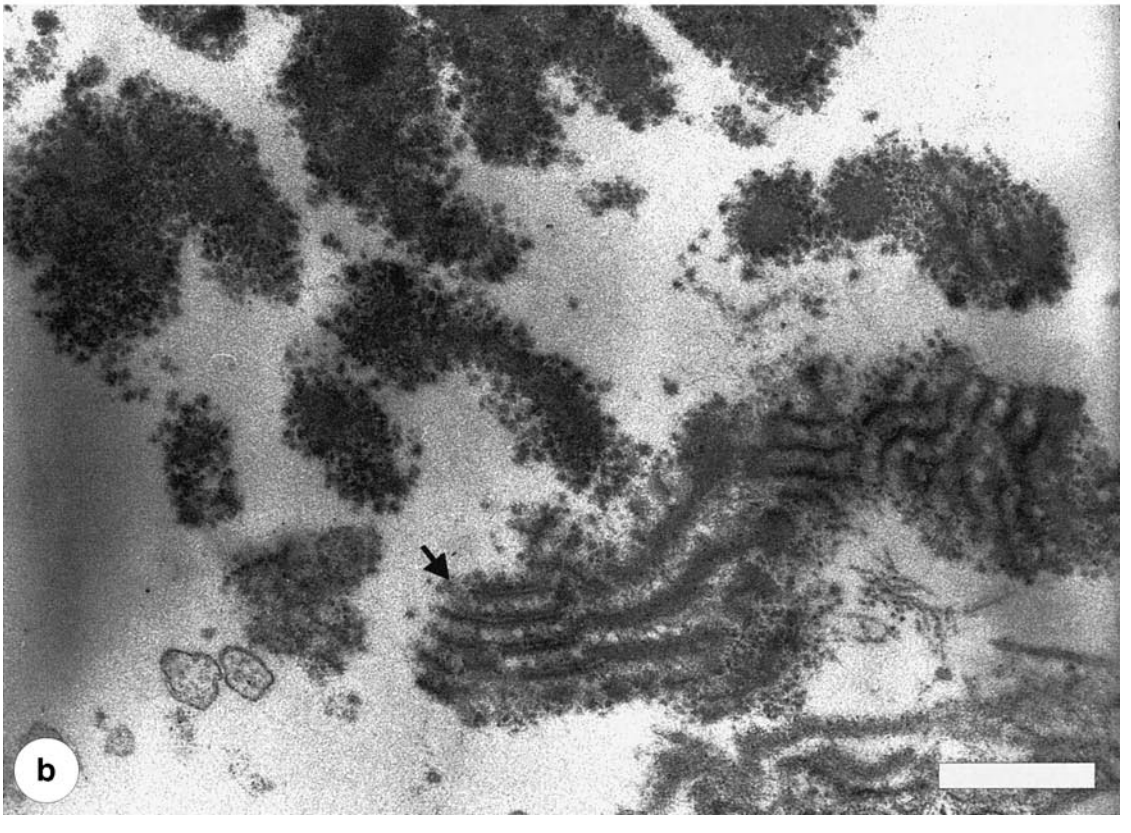
b

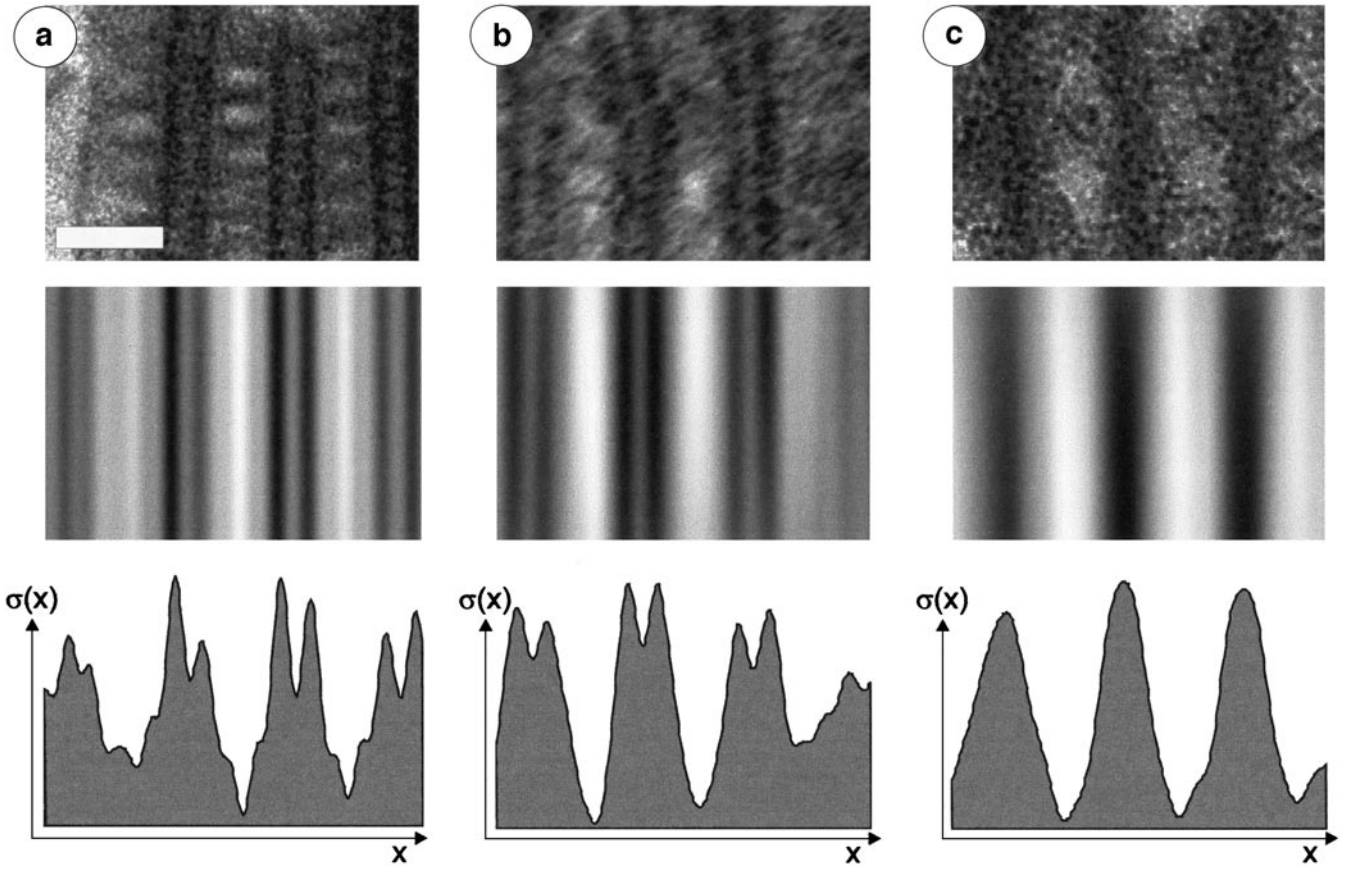


**FIG. 2.** (a) (Top) Portion of the collagen VI assemblies found in the cortical vitreous of a patient with full thickness macular holes (Knupp *et al.*, 2000). (Middle) One-dimensional average obtained by masking and floating the meridional reflections of the Fourier transform of the first panel. (Bottom) Projection onto *x*-axis of the average protein density in the middle panel. Peaks correspond to higher protein density. (b) As in (a) but using the double-banded aggregates found in eyes affected by Sorsby's fundus dystrophy. (c) As in (a) and (b) but using the single-banded aggregates found in association with Sorsby's fundus dystrophy. Bar, 100 nm. All panels are shown at the same absolute magnification.

it was not possible to produce high-resolution averaged images, we could see a considerable amount of detail in the original micrographs. For example, beaded filaments of the kind described by Bruns (1984) for collagen VI could be seen around the aggregates (Figs. 3a–3c). Further, globular assemblies with a double periodicity of about 100 nm could be seen touching the aggregates (Figs. 3d and 3e). These globular assemblies possess the periodicity expected if they were generated by the globular domains of collagen VI beaded filaments.

In order to test whether the images in Figs. 2b and 2c were different views from the same structure and to explain the presence of single- and double-banded aggregates, a further set of experiments was carried out. In the microscope, a broad-banded aggregate was tilted by up to 60° in both directions around a tilt axis that was parallel to the bands themselves. At high angles, in both directions, the bands narrowed to 50% of the original width. At the same time the periodicity of the axial repeat also diminished to less than 80 nm. This is consistent with our model since the collagen VI globular domains would form parallel sheets that run perpendicular to the longitudinal views examined in this study. Once projected onto the *x*-axis (Fig. 4a, first panel), the bands

**FIG. 1.** (a) Typical appearance of the molecular aggregates found in Bruch's membrane of a case of Sorsby's fundus dystrophy. These aggregates are characterized by transverse bands of protein density that repeat axially with a periodicity of about 100 nm. Axial filaments of protein density can also be seen but it is not possible to recognize any regularity in their occurrence. (b) Alternative appearance of the molecular aggregates in Sorsby's fundus dystrophy. The transverse single bands are here split into pairs 30 nm apart (arrow). Bars, 500 nm.

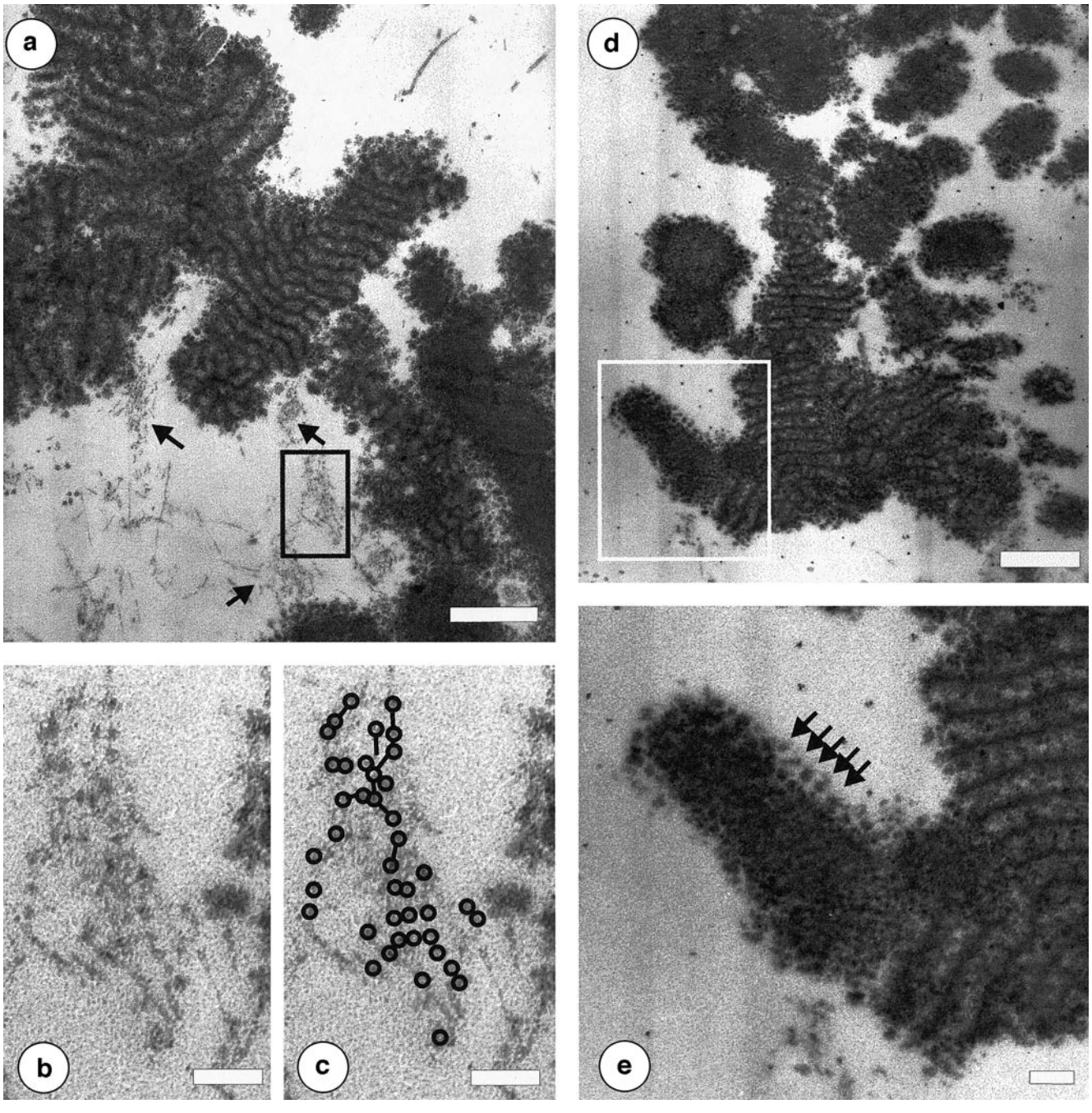


**FIG. 3.** (a) Low-magnification view of one of the assemblies. Arrows point to beaded filaments of the type described by Bruns (1984) for collagen VI. Bar, 500 nm. The boxed region is magnified in (b) and in (c) where the collagen VI globular domains are highlighted by circles. Bars, 100 nm. (d) Low-magnification view of another region of Bruch's membrane. Bar, 500 nm. (e) Magnified view of the boxed region in (d). Globular domains with a double periodicity of about 100 nm can be seen around and on the assemblies. Bar, 100 nm.

give rise to broad rectangular peaks of protein density with a repeat of 100 nm. This density distribution is what is recorded in the microscope. If tilted by 20° in the microscope (Fig. 4a, second panel), the projection of the same bands starts narrowing, giving rise to a trapezoidal protein density distribution, with the center being denser than the periphery. Already at 40° (Fig. 4a, third panel), the bands are much narrower, with a sharp protein density distribution. Such a distribution would appear as a narrow band in the microscope. The axial periodicity also appears reduced. In Fig. 4b we repeated the

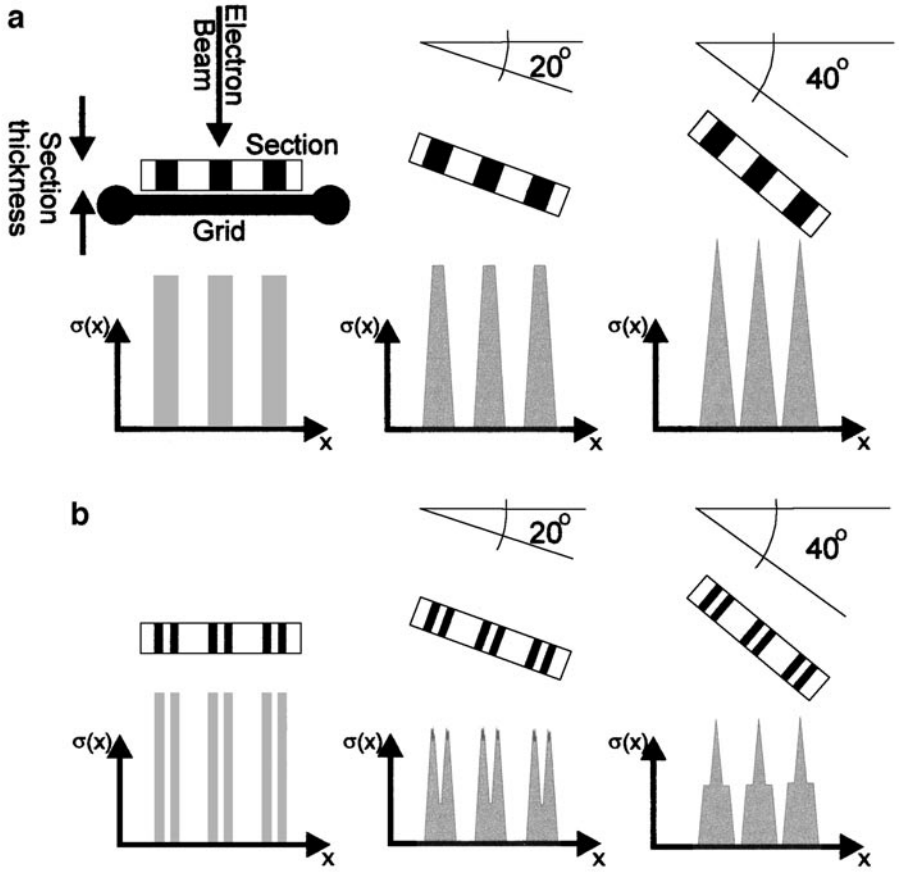


**FIG. 4.** Scheme explaining broad and narrow bands seen in the microscope and that single-banded and double-banded structures with a long repeat are not different views of the same structure. The globular ends of the collagen VI proteins form parallel sheets that run perpendicular to the longitudinal views examined in this study. The gaps between the sheets can be filled with TIMP-3 (a) or be empty (b). The protein density distribution is projected onto the *x*-axis, which runs perpendicular to the electron beam. Higher protein density appears as darker areas on the microscope screen. (a) (First panel) At 0° tilt the protein density appears as broad rectangular peaks repeated every 100 nm. (Second and third panels) at 20° and 40° the recorded protein density from the bands starts sharpening and is viewed in the microscope as narrow bands. The axial periodicity along the *x*-axis is decreasing as well. (b) As in (a) but from double-banded aggregates. Although at high-tilt angles the aggregates appear as single narrow bands (third panel), this is not the case at low-tilt angles (first and second panels). This substantiates the observations that there are two kinds of aggregates present in Sorsby's fundus dystrophy.

same exercise with double-band aggregates. Although at high angles the aggregates appear as single narrow bands (Fig. 4b, third panel), this would also be associated with a marked reduction in the axial periodicity. Tilting of the double-banded aggregates by angles small enough not to greatly alter the periodicity gave images which clearly retained their double-banded character (Fig. 4b, first and second panels). This substantiates the observation that there are two kinds of aggregates present, one giving rise to the broad-band appearances and the other to the double-band appearances.

Very rarely, narrow-banded aggregates, with an axial periodicity of about 100 nm, were noticed. Although these were probably due to either uneven staining or stretching of the plastic sections in the beam, it is not impossible to conceive that they may be due to the aggregation of collagen VI monomers that failed to dimerize due to disulfide bonding of TIMP-3s to the triple-helix cysteines involved in dimerization. Verifying this hypothesis necessitates further investigation.

## DISCUSSION

The very close resemblance of the collagen VI aggregates found in the vitreous of patients suffering from full-thickness macular holes and the double-banded assemblies found in patients suffering from Sorsby's fundus dystrophy leads us to propose that collagen VI is the most probable candidate for formation of the double-banded assemblies. The lack of lateral order in the Sorsby's fundus dystrophy assemblies is not particularly worrying since, occa-

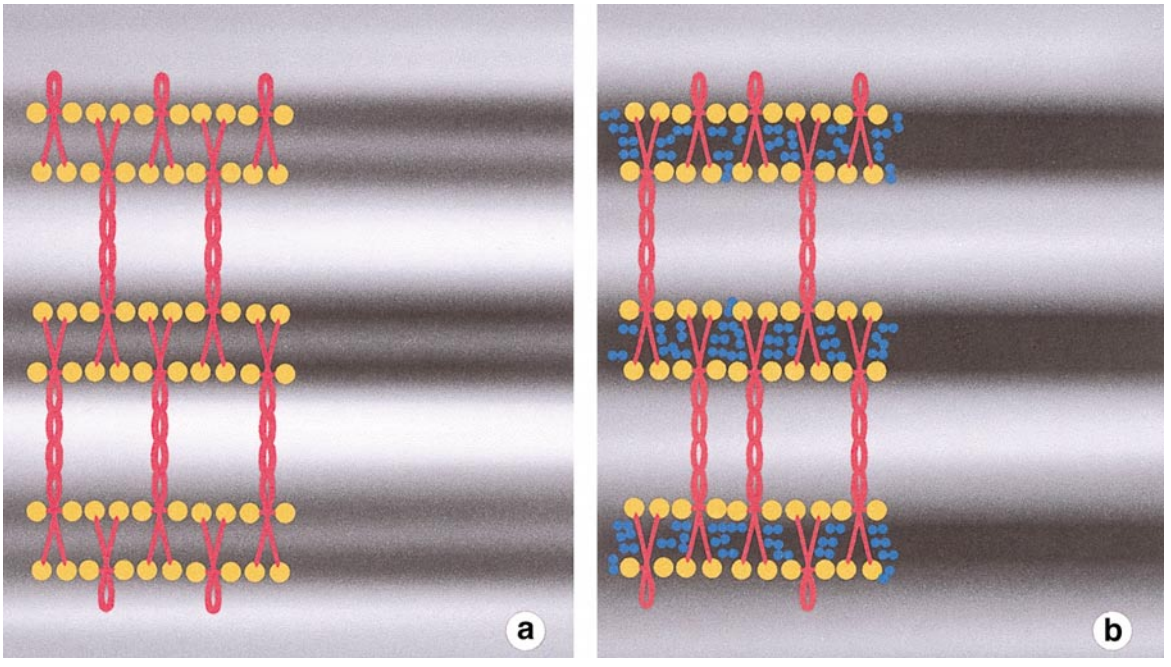


**FIG. 5.** Model for the aggregates in Sorsby's fundus dystrophy. The models are superimposed on the one-dimensional averaged view of the banded appearances. (a) Model for the double-banded appearances. This model is based on collagen VI tetramers. Collagen VI globular domains (depicted in light orange) interact with one another to keep the network together. Since collagen VI monomers assemble with a 30-nm axial shift to form dimers, the massive globular domains are spaced 30 nm apart and give rise, at low resolution, to the double bands seen in the microscope. (b) Model for the single-band appearance. This model is essentially the same as that for the double-band appearances, but with TIMP-3 binding either to the globular domains or to the 30-nm-long triple-helical segment between the globular domains. Accumulation of TIMP-3 in this area would explain why single bands arise in place of double bands.

sionally, this was found to be true also for the vitreous aggregates. A model for the collagen VI assembly in this type of aggregate is illustrated in Fig. 5a. This model is based on collagen VI tetramers. The collagen VI globular domains (depicted in light orange) interact with each other to keep the network together. Since collagen VI monomers assemble with a 30-nm axial shift to form dimers, the massive globular domains end up 30 nm apart and give rise, at low resolution, to the double banding seen in the microscope.

Further evidence about the role of collagen VI in the Sorsby's fundus dystrophy aggregates is given by the presence of collagen VI beaded filaments around the aggregates themselves. It is feasible that the formation of beaded filaments may be one of the transition phases before assembly into the final collagen VI networks seen in the microscope.

Single-band aggregates can also be explained in terms of collagen VI dimers and tetramers. Since the width of single bands corresponds to the width of double bands, the simplest supposition is that there is some extra material occupying the space between the globular domains generating the double bands.

It is known that Sorsby's fundus dystrophy is characterized by a genetic mutation of *TIMP-3* that introduces an additional cysteine in TIMP-3. This leads to the formation of TIMP-3 dimers (Langton *et al.*, 2000). This mutation does not affect the MMP inhibitory activity of TIMP-3 or its ability to bind to extracellular matrix. In addition TIMP-3 was found to be present in the Sorsby's fundus dystrophy deposits by immunohistochemistry (Fariss *et al.*, 1998; Chong *et al.*, 2000). Our structural observations can be simply explained if mutated TIMP-3 binds either to the collagen VI globular domains or to the 30-nm-long segment of the triple-helix situated between the globular domains in collagen VI dimers and tetramers. Thus abnormally bound TIMP-3 could be protected from normal metabolic processes and its natural turnover slowed considerably. In turn, TIMP-3 could itself be shielding collagen VI assemblies from degradation.

Figure 5b shows a model of the proposed molecular assembly of collagen VI in Sorsby's fundus dystrophy aggregates. Tetramers are assembling through their globular domains (depicted in light orange). Occasionally, this globular domain interaction could be hindered by the presence of TIMP-3 dimers and local disruption may occur with a consequent increase in irregularity of the collagen VI assembly. This would explain the lack of order in the

single-banded aggregates seen in the microscope. The presence of both double-banded and single-banded aggregates can be explained by different amounts of TIMP-3 binding.

The balance of TIMPs and MMPs regulates remodeling of the extracellular matrix, playing a role in physiological processes as diverse as embryonic development, wound healing, glandular morphogenesis, and angiogenesis. A TIMP–MMP imbalance due to abnormal TIMP-3 binding to collagen VI may initiate a chain of events that leads to fundus dystrophy and to blindness.

## CONCLUSIONS

The structural analysis carried out in this work leads us to the conclusion that collagen VI is responsible for the banded assemblies seen in Bruch's membrane of patients suffering from Sorsby's fundus dystrophy. Furthermore, a tentative role for TIMP-3 in the disease has also been proposed. In fact, disruption of the normal metabolic processes in the retina may well occur as a consequence of collagen VI–TIMP-3 binding, and reduced retinal sensitivities may be a product of this disruption. Further work is necessary to substantiate this hypothesis.

Assemblies of the kind described in this study are also present in eyes suffering from age-related macular degeneration. Progress in the understanding of the pathophysiology of this common disease may be linked to the understanding of the collagen assemblies associated with it, and the understanding of the aggregates in Sorsby's fundus dystrophy represents a step forward in this direction.

C.K. and J.M.S. acknowledge support from the Wellcome Trust (0389048). The Jeol 1200 EX microscope was also purchased with a grant from the Wellcome Trust (14480).

## REFERENCES

Ayad, S., Boot-Hanford, R. P., Humphries, M. J., Kadler, K. E., and Shuttleworth, C. A. (1994) The Extracellular Matrix Facts Book, Academic Press, San Diego.

Bird, A. (1992) Bruch's membrane changes with age. *Br. J. Ophthalmol.* **763,** 166–168.

Bruns, R. R. (1984) Beaded filaments and long-spacing fibrils: Relation to type VI collagen. *J. Ultrastruct. Res.* **89,** 136–145.

Chong, N. H. V., Alexander, R. A., Gin, T., Bird, A. C., and Luthert, P. J. (2000) TIMP-3, collagen and elastin immunohistochemistry and histopathology of Sorsby's fundus dystrophy. *Invest. Ophthalmol. Vis. Sci.* **41,** 898–902.

Crowther, R. A., Henderson, R., and Smith, J. M. (1996) MRC image processing programs. *J. Struct. Biol.* **116,** 9–16.

Fariss, R. N., Apte, S. S., Olsen, B. R., Iwata, K., and Milam, A. H. (1997) Tissue inhibitor of metalloproteinase is a component of Bruch's membrane of the eye. *Am. J. Pathol.* **150,** 323–328.

Fariss, R. N., Apte, S. S., Luthert, P. J., Bird, A. C., and Milam, A. H. (1998) Accumulation of tissue inhibitor of metalloproteinases-3 in human eyes with Sorsby's fundus dystrophy or retinitis pigmentosa. *Br. J. Ophthalmol.* **82,** 1329–1334.

Feeney-Burns, L., and Ellersieck, M. (1985) Age-related changes in the ultrastructure of Bruch's membrane. *Am. J. Ophthalmol.* **100,** 686–697.

Feher, J., and Valu, L. (1967) On the structure of Bruch's membrane. *Albrecht Von Graefes Arch. Klin. Exp. Ophthalmol.* **173**(2), 162–167.

Felbor, U., Stohr, H., Amann, T., Schonherr, U., and Weber, B. H. F. (1995) A novel Ser156Cys mutation in the tissue inhibitor of metalloproteinase-3 (TIMP-3) in Sorsby's fundus dystrophy with unusual clinical features. *Hum. Mol. Genet.* **4,** 2415–2416.

Felbor, U., Doepner, D., Schneider, U., Zrenner, E., and Weber, B. H. (1997) Evaluation of the gene encoding the tissue inhibitor of metalloproteinases-3 in various maculopathies. *Invest. Ophthalmol. Vis. Sci.* **38,** 1054–1059.

Furthmayr, H., Wiedemann, H., Timpl, R., Odermatt, E., and Engel, J. (1983) Electron microscopical approach to a structural model of intima collagen. *Biochem. J.* **211,** 303–311.

Guo, L., Hussain, A., Kundaiker, S., and Marshall, J. (1997) Metalloproteinase activity of human Bruch's membrane-choroid samples as a function of age. *IOVS Suppl.* **38,** S354.

Guymer, R., and Bird, A. C. (1998) Bruch's membrane, drusen, and age-related macular degeneration. *In* Marmor, M. F. and Wolfensberger, T. J. (Eds.), The Retinal Pigment Epithelium, pp. 693–705, Oxford Univ. Press, New York.

Hewitt, A., Nakazawa, K., and Newsome, D. (1989) Analysis of newly synthesized Bruch's membrane proteoglycans. *Invest. Ophthalmol. Vis. Sci.* **30,** 478–486.

Hodgetts, A., Hussain, A. A., Starita, C., Hageman, G. S., and Marshall, J. (1998a) Morphological and biochemical factors regulating fluid transport through Bruch's membrane and their implications for the ageing process. *Exp. Eye Res. Suppl.*, p. 67.

Hodgetts, A., Hussain, A. A., Hageman, G. S., and Marshall, J. (1998b) Effect of enzymatic modulation on the hydrodynamics of ageing human Bruch's membrane. *Invest. Ophthalmol. Vis. Sci. Suppl.* **39,** 369.

Holz, F., Wolfensberger, T., Piguet, B., Gross-Jendroska, M., Wells, J., Minassian, D., Chisholm, I., and Bird, A. (1994a) Bilateral macular drusen in age-related macular degeneration. Prognosis and risk factors. *Ophthalmology* **101**(9), 1522–1528.

Holz, F., Sheraiadah, G., Pauleikhoff, D., Marshall, J., and Bird, A. (1994b) Analysis of lipid deposits extracted from human macular and peripheral Bruch's membrane. *Arch. Ophthalmol.* **112,** 402–406.

Ishibashi, T., Toshinori, M., Hangai, M., Nagai, R., Horiuchi, S., Lopez, P. F., Hinton, D. R., and Ryan, S. J. (1998) Advanced glycation end products in age-related macular degeneration. *Arch. Ophthalmol.* **116,** 1629–1632.

Jacobson, S. G., Cideciyan, A. V. and Regunath, G. (1995) Night blindness in Sorsby's fundus dystrophy reversed by vitamin A. *Nat. Genet.* **11,** 27–32.

Kamei, M., and Hollyfield, J. G. (1999) TIMP-3 in Bruch's membrane: Changes during aging and age-related macular degeneration. *Invest. Ophthalmol. Vis. Sci.* **40,** 2367–2375.

Karwatowski, W. S., Jeffries, T. E., Duance, V. C., Albon, J., Bailey, A. J., and Easty, D. L. (1995) Preparation of Bruch's membrane and analysis of the age-related changes in the structural collagens. *Br. J. Ophthalmol.* **79**(10), 944–952.

Knupp, C., Munro, P. J., Luther, P. K., Ezra, E., and Squire, J. M. (2000) Structure of abnormal assemblies (collagen VI) associated with human full thickness macular holes. *J. Struct. Biol.* **129,** 38–47.

Knupp, C., and Squire, J. M. (2001) A new twist in the collagen story: The type VI segmented supercoil. *EMBO J.* **20**(3), 372–376.

Kuo, H-J., Keene, D. R., and Glanville, R. W. (1995) The macromolecular structure of type VI collagen formation and stability of filaments. *Eur. J. Biochem.* **232,** 364–372.

Langton, K. P., McKie, N., Curtis, A., Goodship, J. A., Bond, P. M., Barker, M. D., and Clarke, M. A. (2000) Novel TIMP-3 mutation reveals a common molecular phenotype in Sorsby's fundus dystrophy. *J. Biol. Chem.* **275,** 27027–27031.

Langton, K. P., Barker, M. D., and McKie, N. (1998) Localization of the functional domains of human tissue inhibitor of metalloproteinases-3 and the effects of a Sorsby's fundus dystrophy mutation. *J. Biol. Chem.* **273,** 16779–16781.

Marshall, J., Hussain, A. A., Starita, C., Moore, D. J., and Patmore, A. L. (1998) Aging and Bruch's membrane. *In* Marmor, M. F. and Wolfensberger, T. J. (Eds.), The Retinal Pigment Epithelium, pp. 669–692, Oxford Univ. Press, New York.

Misell, D. L. (1978) Image analysis and interpretation. *In* Glauert, A. M. (Ed.), Practical Methods in Electron Microscopy, pp. 125–179, Elsevier/North-Holland, Amsterdam.

Moore, D., Hussain, A., and Marshall, J. (1995) Age-related variation in the hydraulic conductivity of Bruch's membrane. *Invest. Ophthalmol. Vis. Sci.* **36,** 1290–1297.

Newsome, D., Hewitt, A., Huh, W., Robey, P., and Hassell, J. (1987a) Detection of specific extracellular matrix molecules in drusen, Bruch's membrane, and ciliary body. *Am. J. Ophthalmol.* **104,** 373–381.

Newsome, D., Huh, W., and Green, W. (1987b) Bruch's membrane age-related changes vary by region. *Curr. Eye Res.* **6,** 1211–1221.

Opdenakker, G., and Van Damme, J. (1992) Cytokines and proteases in invasive processes: Molecular similarities between inflammation and cancer. *Cytokine* **4,** 251–258.

Pauleikhoff, D., Barondes, M., Minassian, D., Chisholm, I., and Bird, A. (1990) Drusen as risk factors in age-related macular disease. *Am. J. Ophthalmol.* **109,** 38–43.

Paulcikhoff, D., Zuels, S., Sheraidah, G., Marshall, J., Wessing, A., and Bird, A. (1992) Correlation between biochemical composition and fluorescein binding of deposits in Bruch's membrane. *Ophthalmology* **99,** 1548–1553.

Ramrattan, R., van der Schaft, T., Mooy, C., de Bruijn, W., Mulder, P., and de Jong, P. (1994) Morphometric analysis of Bruch's membrane, the choriocapillaris, and the choroid in aging. *Invest. Ophthalmol. Vis. Sci.* **35,** 2857–2864.

Reale, E., Groos, S., Luciano, L., Eckardt, C., and Eckardt, U. (2001) In the mammalian eye type VI collagen forms three morphologically different aggregates. *Matrix Biol.* **20,** 37–51.

Ruiz, A., Brett, P., and Bok, D. (1996) TIMP-3 is expressed in human retinal pigment epithelium. *Biochem. Biophys. Res. Commun.* **226,** 467–474.

Sheraidah, G., Steinmetz, R., Maguire, J., Pauleikhoff, D., Marshall, J., and Bird, A. (1993) Correlation between lipids extracted from Bruch's membrane and age. *Ophthalmology* **100,** 47–51.

Spraul, C., and Grossniklaus, H. (1997) Characteristics of drusen and Bruch's membrane in postmortem eyes with age-related macular degeneration. *Arch. Ophthalmol.* **115,** 267–273.

Starita, C., Hussain, A., Pagliarini, S., and Marshall, J. (1996) Hydrodynamics of ageing Bruch's membrane: Implications for macular disease. *Exp. Eye Res.* **62,** 565–572.

Von Der Mark, H., Aumailley, M., Wick, G., Fleischmayer, R., and Timpl, R. (1984) Immunochemistry, genuine size and tissue localisation of collagen VI. *Eur. J. Biochem.* **142,** 243–502.

Vranka, J. A., Johnson, E., Zhu, X., Shepardson, A., Alexander, J. P., Bradley, J. M., Wirtz, M. K., Weleber, R. G., Klein, M. L., and Acott, T. S. (1997) Discrete expression and distribution pattern of TIMP-3 in the human retina and choroid. *Curr. Eye Res.* **16**(2), 102–110.

Weber, B. H. F., Vogt, G., Pruett, R. C., Stohr, H., and Felbor, U. (1994) Mutations in the tissue inhibitor of metalloproteinase-3 (TIMP-3) in patients with Sorsby's fundus dystrophy. *Nat. Genet.* **8,** 352–356.

Wu, J-J., Eyre, D. R., and Slayter, H. S. (1987) Type VI collagen of the invertebral disc. *Biochem. J.* **248,** 373–381.